

Kinematic distributions of the η_c leptonproduction in association with light hadrons

Hong-Fei Zhang,^a Xue-Mei Mo^a

^a*Guizhou University of Finance and Economics, Guiyang, 550025, China*

E-mail: shckm2686@163.com, dmtmmu@163.com

ABSTRACT: The η_c meson leptonproduction is calculated within the nonrelativistic QCD framework for the first time. It is found that the colour-singlet channel, although suppressed by a factor of α_s relative to the colour-octet ones, provides the important contribution for almost all the experimental conditions, which disagrees with some of the expectations before computation. We present the differential cross sections with respect to p_t^2 , p_t^{*2} , Q^2 , W , and z , for both HERA and EIC experimental conditions as a reference for future studies. The scale dependence and long-distance-matrix-element dependence are also investigated in this paper.

KEYWORDS: Deep inelastic scattering, Nonrelativistic QCD

Contents

1	Introduction	1
2	Analytic Framework	3
3	Numerical Results	5
3.1	Results for HERA experiment	7
3.2	Results for EIC experiment	7
3.3	Scale dependences	7
3.4	Long-distance-matrix-element dependence	9
4	Summary	12

1 Introduction

The quarkonium production mechanism is a puzzle hanging for decades. In 1994, the colour-octet mechanism [1] was proposed to explain the significant discrepancy between theory and the measurement of the J/ψ hadroproduction carried out at the Tevatron [2]. Although this discrepancy was mended by an extremely large short-distance coefficient of the $c\bar{c}(^3S_1^{[8]})$ hadroproduction [3], some new troubles emerge and further efforts were devoted to both theoretical computations and experimental measurements. Among the difficulties, a well-known one is the J/ψ polarization puzzle, i.e. the Tevatron measurement [4] of the J/ψ polarization contradicts the $^3S_1^{[8]}$ -dominance picture, in which most of the J/ψ 's are produced through one-gluon fragmentation and thus the longitudinal polarization is greatly suppressed. It was not until the next-to-leading order calculations was achieved did physicists find possibilities to solve this puzzle. The behavior of the $^3P_J^{[8]}$ short-distance coefficients are completely changed at QCD next-to-leading order [5–8], which leads to new values of the long-distance matrix elements that disfavor the $^3S_1^{[8]}$ dominance picture. Three groups calculated the QCD corrections to the J/ψ hadroproduction and studied its polarization [9–11], however, with different fitting strategies, they got completely different values of the long-distance matrix elements, and their perspectives on the J/ψ polarization puzzle were also different. As pointed out in Reference [12], the J/ψ production data alone can not fix all the three long-distance matrix elements. A milestone was the measurement of the η_c hadroproduction [13, 14], which, provides unique information for the charmonia production, and, by virtue of heavy quark spin symmetry, can help to eliminate the degrees of freedom in the fit of the long-distance matrix elements for the J/ψ production [15, 16]. It is demonstrated in Reference [12] that the J/ψ and η_c hadroproduction data along with the J/ψ polarization data at hadron colliders can be well described with one set of long-distance matrix elements. Unfortunately, the theoretical results using this set of parameters

disagree with the Belle data [17, 18]; there does not exist any set of long-distance matrix elements that can describe all the existing data.

Inspired by the fact that the QCD corrections to quarkonium production processes are usually remarkable, some people expect that the next-to-next-to-leading-order correction to the colour-singlet channel might also be important [19], and thus the colour-octet long-distance matrix elements might have been overestimated. They sought the possibility to interpret the existing data in the absence of the colour-octet contributions and found that the experimental data of some processes, e.g. the J/ψ production at B-factories [20–22], is saturated by the colour-singlet channel. In order to clarify this puzzling problem, it is important to find out more processes of which the colour-singlet contributions are negligible compared to the colour-octet ones. In Reference [23], the authors studied the η_c photoproduction in electron-proton collisions and found that, in the direct photon processes, the colour-singlet channel is 1-2 orders of magnitude smaller than the colour-octet ones. However, this feature is ruined by the resolved-photon contributions which enhance the colour-singlet part by two orders of magnitude.

In this paper, we study the η_c production in deep inelastic electron-proton (ep) scattering. In this process, the resolved-photon contributions are negligible, at the same time, the good feature, namely the colour-singlet 1S_0 $c\bar{c}$ is produced with at least two gluons emitted, is retained. Although the short-distance coefficient for the colour-singlet process is suppressed by a factor of α_s comparing with the colour-octet ones, the colour-singlet long-distance matrix element is enhanced by some powers of $1/v$. Since for the charmonia, v^4 is approximated to be 0.1, one cannot naively conclude a colour-octet dominance picture in the η_c photoproduction just from the analysis of the scaling. This process was first investigated in Reference [24]. However, as pointed out in References [25, 26], there might be some mistakes in the calculations of the quarkonium leptoproduction at that time, and in any case, the results for the colour-singlet channel was not given in Reference [24]. As a matter of fact, this process is quite complicated due to the nonzero invariant mass of the initial photon, which can be seen from the fact that the first correct complete nonrelativistic-QCD result for the J/ψ leptoproduction at QCD leading order was obtained in Reference [26] in as late as 2017; the first QCD next-to-leading-order result of the colour-singlet J/ψ production was completed in 2017 [27], while the parallel results for the J/ψ photoproduction was published more than ten years ago [28]; and its colour-octet counterparts are still lacking. This paper will, for the first time, present the complete results of the η_c leptoproduction within the nonrelativistic QCD framework, and discuss the possibility of distinguishing the colour-singlet and colour-octet mechanisms using this process. The experimental data can be obtained by revisiting of the HERA data. Further, we suggest it be measured in the future Electron-Ion Collider (EIC).

In Section 2 we outline the calculation framework. Having the essential analytical formulas, we present the numerical results in Section 3. A concluding remark is presented in the last section.

2 Analytic Framework

The process studied in this paper can be illustrated as

$$p(P) + e(k) \rightarrow \eta_c(p) + X + e(k'), \quad (2.1)$$

which can be accessed through the evaluation of the following process,

$$p + \gamma^*(q) \rightarrow \eta_c + X, \quad (2.2)$$

where p , e , and γ^* denote the proton, electron, and off-shell photon, respectively, and X can be any hadronic final states. The effects of the initial protons can be further factorized as partonic processes convolved with the parton-distribution functions, while the η_c production can be factorized, according to nonrelativistic QCD [1], as the production of the intermediate $c\bar{c}$ states (the short-distance coefficients) multiplied by the process-independent nonperturbative parameters (the long-distance matrix elements). The factorization can be illustrated as

$$d\sigma(p + \gamma^* \rightarrow \eta_c + X) = \sum_{i,n} \int dx f_{i/p}(x, \mu_f) d\hat{\sigma}(i + \gamma^* \rightarrow c\bar{c}[n] + X) \langle \mathcal{O}^{\eta_c}(n) \rangle, \quad (2.3)$$

where i runs over all possible species of partons, namely gluon, u , d , and s quarks, n denotes the quantum number of the intermediate $c\bar{c}$ state, and $f_{i/p}(x, \mu_f)$ is the parton-distribution function at the factorization scale μ_f . The momentum of the initial parton, p_i can be evaluated as $p_i = xP$. For the η_c production, four intermediate $c\bar{c}$ states are involved up to the order $\mathcal{O}(v^4)$, where v is the typical relative velocity of the charm quarks in the η_c mesons, they are $c\bar{c}[^1S_0^{[1]}]$, $c\bar{c}[^1S_0^{[8]}]$, $c\bar{c}[^3S_1^{[8]}]$, and $c\bar{c}[^1P_1^{[8]}]$.

The leading-order process for the $c\bar{c}[^1S_0^{[8]}]$ production is

$$g + \gamma^* \rightarrow c\bar{c}[^1S_0^{[8]}], \quad (2.4)$$

which is of order $\mathcal{O}(\alpha\alpha_s)$. Here, g denotes a gluon, and α and α_s are the electroweak and strong couplings, respectively. If we impose a cut-off on the transverse momentum of η_c (p_t^*), this process will not be observed. Here and in the following, we use the superscript \star to denote the kinematic variables in the proton-photon centre-of-mass frame. The leading order processes for the production of the colour-octet intermediate states with nonzero p_t^* are listed below,

$$\begin{aligned} g + \gamma^* &\rightarrow c\bar{c}[^1S_0^{[8]}] + g, \\ q + \gamma^* &\rightarrow c\bar{c}[^1S_0^{[8]}] + q, \\ g + \gamma^* &\rightarrow c\bar{c}[^3S_1^{[8]}] + g, \\ q + \gamma^* &\rightarrow c\bar{c}[^3S_1^{[8]}] + q, \\ g + \gamma^* &\rightarrow c\bar{c}[^1P_1^{[8]}] + g, \end{aligned} \quad (2.5)$$

where q denotes a light quark (u , d , s). The leading-order process to produce a colour-singlet η_c is

$$g + \gamma^* \rightarrow c\bar{c}[^1S_0^{[1]}] + g + g. \quad (2.6)$$

Denoting the momenta of the initial proton and electron, the short-distance coefficients for the processes listed above can be written as

$$d\hat{\sigma}(i + \gamma^* \rightarrow c\bar{c}[n] + X) = \frac{1}{2xS} \frac{1}{N_s N_c} \frac{1}{(Q^2)^2} L_{\mu\nu} H^{\mu\nu}(i + \gamma^* \rightarrow c\bar{c}[n] + X) d\Phi, \quad (2.7)$$

where S and Q^2 are defined in terms of the following equation,

$$S = (P + k)^2 \approx 2P \cdot k, \quad Q^2 = (k - k')^2, \quad (2.8)$$

$1/(N_s N_c)$ is the colour and spin average factor, $L_{\mu\nu}$ and $H^{\mu\nu}$ are the leptonic and hadronic tensors, respectively, and $d\Phi$ is the phase space.

Having the definition of the following invariants,

$$W^2 = (P + q)^2, \quad y = \frac{W^2 + Q^2}{S}, \quad z = \frac{P \cdot p}{P \cdot q}, \quad (2.9)$$

the leptonic tensor can be expressed as

$$L_{\mu\nu} = 8\pi\alpha Q^2 l_{\mu\nu}, \quad (2.10)$$

with

$$l^{\mu\nu} = A_g(-g^{\mu\nu} - \frac{q^\mu q^\nu}{Q^2}) + A_L \epsilon_L^\mu \epsilon_L^\nu + A_T \epsilon_T^\mu \epsilon_T^\nu + A_{lt}(\epsilon_t^\mu \epsilon_t^\nu + \epsilon_t^\mu \epsilon_l^\nu). \quad (2.11)$$

where

$$\begin{aligned} \epsilon_t &= \frac{1}{Q} \left(q + \frac{2Q^2}{s} p_i \right), \\ \epsilon_l &= \frac{1}{p_t^*} (p - \rho p_i - zq), \end{aligned} \quad (2.12)$$

and

$$\begin{aligned} A_g &= 1 + \frac{2(1-y)}{y^2} - \frac{2(1-y)}{y^2} \cos(2\psi^*), \\ A_L &= 1 + \frac{6(1-y)}{y^2} - \frac{2(1-y)}{y^2} \cos(2\psi^*), \\ A_{LT} &= \frac{2(2-y)}{y^2} \sqrt{1-y} \cos(\psi^*), \\ A_T &= \frac{4(1-y)}{y^2} \cos(2\psi^*). \end{aligned} \quad (2.13)$$

Here, ψ^* is the azimuthal angle of η_c in the proton-photon centre-of-mass frame, and

$$\begin{aligned} s &= (p_i + q)^2 + Q^2 = 2p_i \cdot q, \\ m_t^{*2} &= p_t^{*2} + M^2 \\ \rho &= \frac{m_t^{*2}/z + zQ^2}{s}, \end{aligned} \quad (2.14)$$

where M is the η_c mass.

For the colour-octet processes [26],

$$dx f_{i/p}(x) d\Phi = \frac{1}{(4\pi)^4 S(W^2 + Q^2) z(1-z)} f_{i/p}(x) dQ^2 dW^2 dz dp_t^{*2} d\psi^*, \quad (2.15)$$

while for the colour-singlet process, i.e.

$$g(p_i) + \gamma^*(q) \rightarrow c\bar{c}[^1S_0^{[1]}](p) + g(p_1) + g(p_2), \quad (2.16)$$

we have

$$dx f_{i/p}(x, \mu_f) d\Phi = \frac{1}{(4\pi)^7 S(W^2 + Q^2) z(1-z)} f_{i/p}(x) dQ^2 dW^2 dz dp_t^{*2} d\psi^* ds_{12} d\Omega_1, \quad (2.17)$$

where $s_{12} = (p_1 + p_2)^2$, and $d\Omega_1$ is the infinitesimal spatial angle of \mathbf{p}_1 in the p_1 - p_2 centre-of-mass frame.

The results of the hadronic tensors for $c\bar{c}[^1S_0^{[8]}]$ and $c\bar{c}[^3S_1^{[8]}]$ have been given in Reference [26]. The only missing elements are those for $c\bar{c}[^1S_0^{[1]}]$ and $c\bar{c}[^1P_1^{[8]}]$. Since the results for the colour-singlet state is very complicated, we do not present their analytical results. These missing elements are calculated using a new *Mathematica* program. Its validity is checked by the reevaluation of the processes for the production of the $^1S_0^{[8]}$ and $^3S_1^{[8]}$ states.

3 Numerical Results

In our numerical calculations, we adopt the following parameter choices. The default value of the charm quark mass is given as $m_c = 1.5$ GeV, and the fine-structure constant is approximated as $\alpha = 1/137$. The renormalization scale (μ_r) and factorization scale (μ_f) are set to be $\mu_r = \mu_f = \mu_0 \equiv \sqrt{Q^2 + M^2}$, where M is the η_c mass. For the sake of gauge invariance, its value is fixed to $M = 2m_c$. For HERA experiment, the energy of the electron beams is 27.5 GeV and that of the proton beams is 920 GeV, while for the EIC, they are 21 GeV and 100 GeV, respectively. We employ CTEQ6L1 [29] as the PDF for the protons. The CS LDME is computed according to

$$\langle \mathcal{O}^{\eta_c}(^1S_0^{[1]}) \rangle = \frac{3}{2\pi} |R(0)|^2, \quad (3.1)$$

To obtain the value of α_s , one-loop running equation is employed and its value at the Z_0 -boson mass is set to be $\alpha_s(M_Z) = 0.13$. For the HERA experiment, we apply the following kinematic constraints, $4 \text{ GeV}^2 < p_t^{*2} < 100 \text{ GeV}^2$, $4 \text{ GeV}^2 < Q^2 < 100 \text{ GeV}^2$, $60 \text{ GeV} < W < 240 \text{ GeV}$, and $0 < z < 0.6$, respectively, while for the EIC experiment, the constraints are $4 \text{ GeV}^2 < p_t^{*2} < 36 \text{ GeV}^2$, $4 \text{ GeV}^2 < Q^2 < 36 \text{ GeV}^2$, $20 \text{ GeV} < W < 80 \text{ GeV}$, and $0 < z < 0.6$, respectively. In this paper, we calculate the differential cross sections with respect to p_t^2 , p_t^{*2} , Q^2 , W , and z , in the kinematic regions constrained by the conditions given above, excluding that for the observed variable. For instance, the differential cross section with respect to p_t^{*2} is calculated in the region defined by the following constraints, $4 \text{ GeV}^2 < Q^2 < 36 \text{ GeV}^2$, $20 \text{ GeV} < W < 80 \text{ GeV}$, and $0 < z < 0.6$. Note that we use p_t to denote the transverse momentum of η_c measured in the laboratory frame.

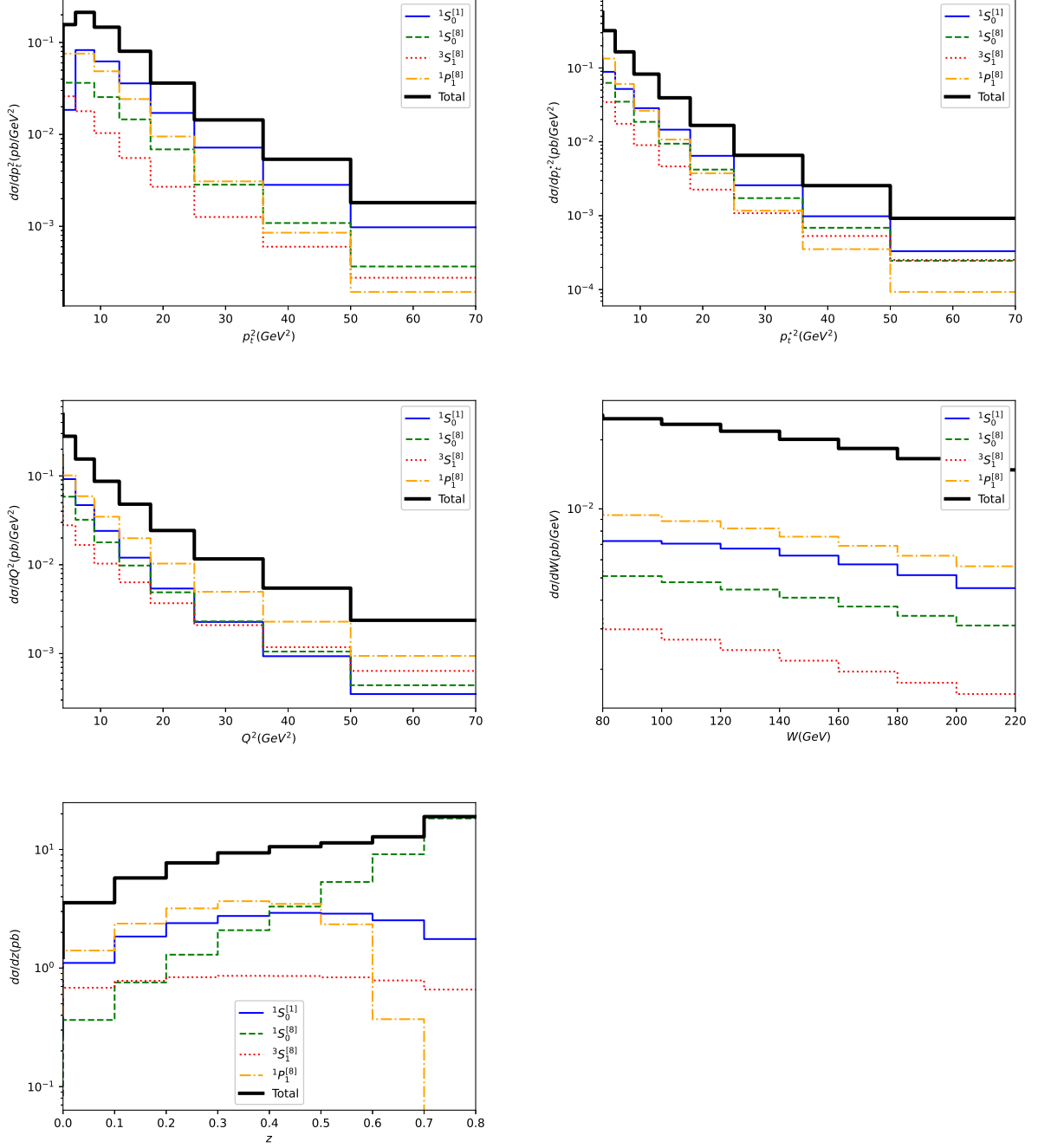


Figure 1: The differential cross sections of the η_c lepton production with respect to p_t^2 , p_t^{*2} , Q^2 , W , and z in HERA experimental condition.

3.1 Results for HERA experiment

The results for the HERA experimental condition are presented in Figure 1, where the long-distance matrix elements are taken from References [12, 16]. Their values are

$$\begin{aligned}
\langle \mathcal{O}^{\eta_c}(^1S_0^{[1]}) \rangle &= 0.16 \text{ GeV}^3, \\
\langle \mathcal{O}^{\eta_c}(^1S_0^{[8]}) \rangle &= 0.36 \times 10^{-2} \text{ GeV}^3, \\
\langle \mathcal{O}^{\eta_c}(^3S_1^{[8]}) \rangle &= 0.74 \times 10^{-2} \text{ GeV}^3, \\
\langle \mathcal{O}^{\eta_c}(^1P_1^{[8]}) \rangle / m_c^2 &= 6.0 \times 10^{-2} \text{ GeV}^3.
\end{aligned} \tag{3.2}$$

In low p_t (p_t^*) regions, the most important contribution comes from the intermediate state $c\bar{c}[^1P_1^{[8]}]$, which is mainly due to a large long-distance matrix element. As p_t (p_t^*) increases, its importance rapidly decreases, and the colour-singlet part, although enduring a small long-distance matrix element comparing to the values obtained via potential model, takes the superiority over all its colour-octet counterparts. This observation is unexpected. People used to consider the colour-singlet contribution to be negligible in this process (see e.g. [24]), which is true in a similar process, the η_c production in ep collisions via direct photons [23]. Although seemingly weird, it is not difficult to understand. As a matter of fact, a term scaling as p_t^{-6} (p_t^{*-6}) arises from the off-shell photon in the colour-singlet η_c production, and vanishes as $Q^2 \rightarrow 0$. This explains why in the η_c photoproduction the colour-singlet differential cross section with respect to p_t suffers a sharper decrease than the $^1S_0^{[8]}$ channel, while in the η_c leptonproduction, these two channels has almost the same p_t (p_t^*) behaviour.

One might notice that when z approaches 1, the cross section for the $^1S_0^{[8]}$ channel grows rapidly. This behaviour is due to an unphysical divergence at the endpoint $z = 1$, and will be greatly suppressed if this divergence is smeared by employing some shape functions. For this reason, we impose a cutoff, $z < 0.6$, when evaluating the differential cross sections with respect to all the other kinematic variables.

Another interesting feature that can be seen in Figure 1 is that each of the four channels has a unique behaviour. For example, the differential cross section with respect to p_t^2 for the $^1S_0^{[1]}$, $^1S_0^{[8]}$, $^3S_1^{[8]}$, and $^1P_1^{[8]}$ channels scale as p_t^{-6} , p_t^{-6} , p_t^{-4} , and p_t^{-8} , respectively, in high p_t limit; the colour-singlet and colour-octet 1S_0 states can be further distinguished in the Q^2 distributions. This feature provides us a very good laboratory to study the long-distance matrix elements for the S-wave charmonia production.

3.2 Results for EIC experiment

In the EIC experimental condition (Figure 2), the cross sections are slightly smaller than the HERA ones, keep all the relative significances of the four channels. Since the EIC will run in much higher luminosity than the HERA experiment, it is promising to expect a high-accuracy measurement of the η_c leptonproduction.

3.3 Scale dependences

We also calculated the integrated cross sections, in the HERA experimental condition, for the four intermediate states with different choices of the of the values of the charm

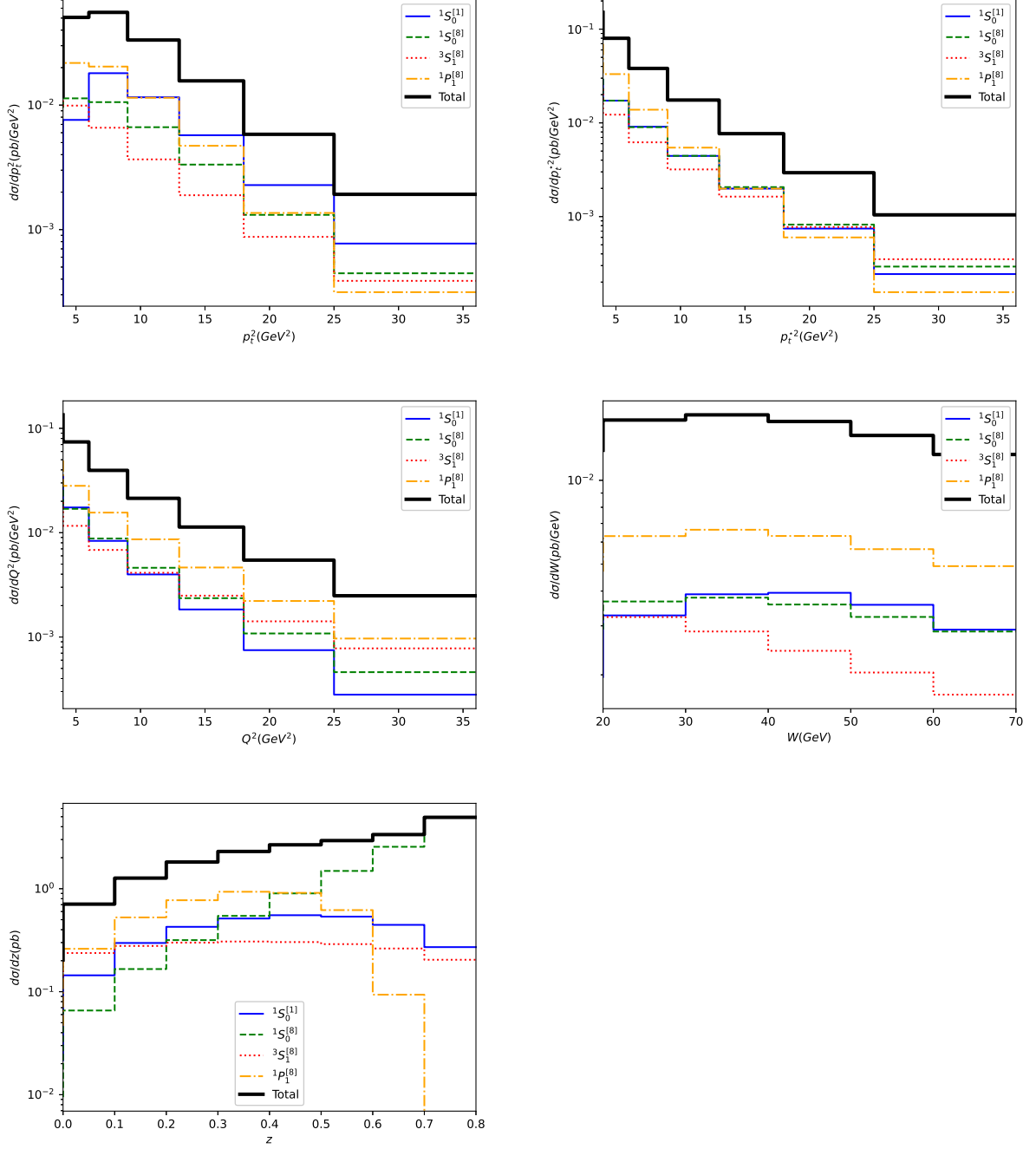


Figure 2: The differential cross sections of the η_c lepton production with respect to p_t^2 , p_t^{*2} , Q^2 , W , and z in EIC experimental condition.

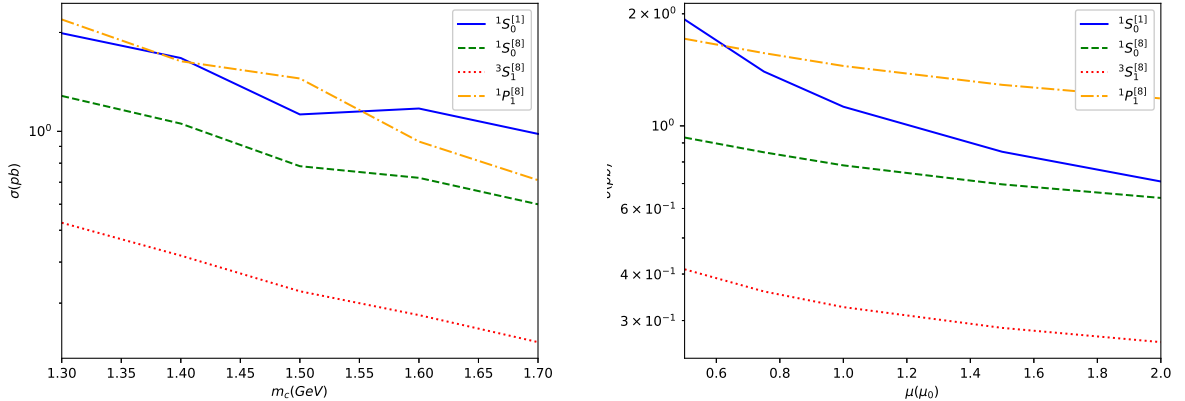


Figure 3: The dependence of the integrated cross section on m_c and $\mu_r = \mu_f = \mu$.

quark mass and the renormalisation and factorisation scales. m_c varies from 1.3 GeV to 1.7 GeV, and $\mu_r = \mu_f = \mu$ varies from $0.5\mu_0$ to $2\mu_0$, where $\mu_0 = \sqrt{Q^2 + M^2}$. The kinematic constraints of the integral follows the conditions given above, namely, $4 \text{ GeV}^2 < p_t^{*2} < 100 \text{ GeV}^2$, $4 \text{ GeV}^2 < Q^2 < 100 \text{ GeV}^2$, $60 \text{ GeV} < W < 240 \text{ GeV}$, and $0 < z < 0.6$. It is found that the scale dependence of the η_c leptonproduction is mild, which indicate good convergence of the perturbative expansions.

3.4 Long-distance-matrix-element dependence

Since there are several sets of long-distance matrix elements available on the market, it is necessary to compare their corresponding predictions and see whether, just like in the J/ψ hadroproduction case, they lead to almost the same results. In the following discussions, we employ five different sets of long-distance matrix elements, taken from References [8, 10, 30, 31], respectively. They are listed in Table 1, excluding our default set which has been given in Equation 3.2. Each of them is independently obtained, and can describe the J/ψ yield data at the Tevatron and LHC. Note that the long-distance matrix elements for the J/ψ production are extracted also in References [11, 32], since the authors of the two references have updated their results in References [30, 31], respectively, we do not present results for the old version of the long-distance matrix elements in this paper.

In Figure 4 and Figure 5, the differential cross sections with respect to the five different kinematic variables are presented for HERA and EIC experimental conditions, respectively. Unlike the J/ψ hadroproduction case, the five sets of long-distance matrix elements lead to different results. This feature has also been observed in the η_c photoproduction [23]. For all the distributions, the long-distance matrix elements taken from References [10, 30] give almost the same results, since both of them are dominated by the 3S_1 colour-octet channel. The other three independent results can be easily distinguished in any of the plots.

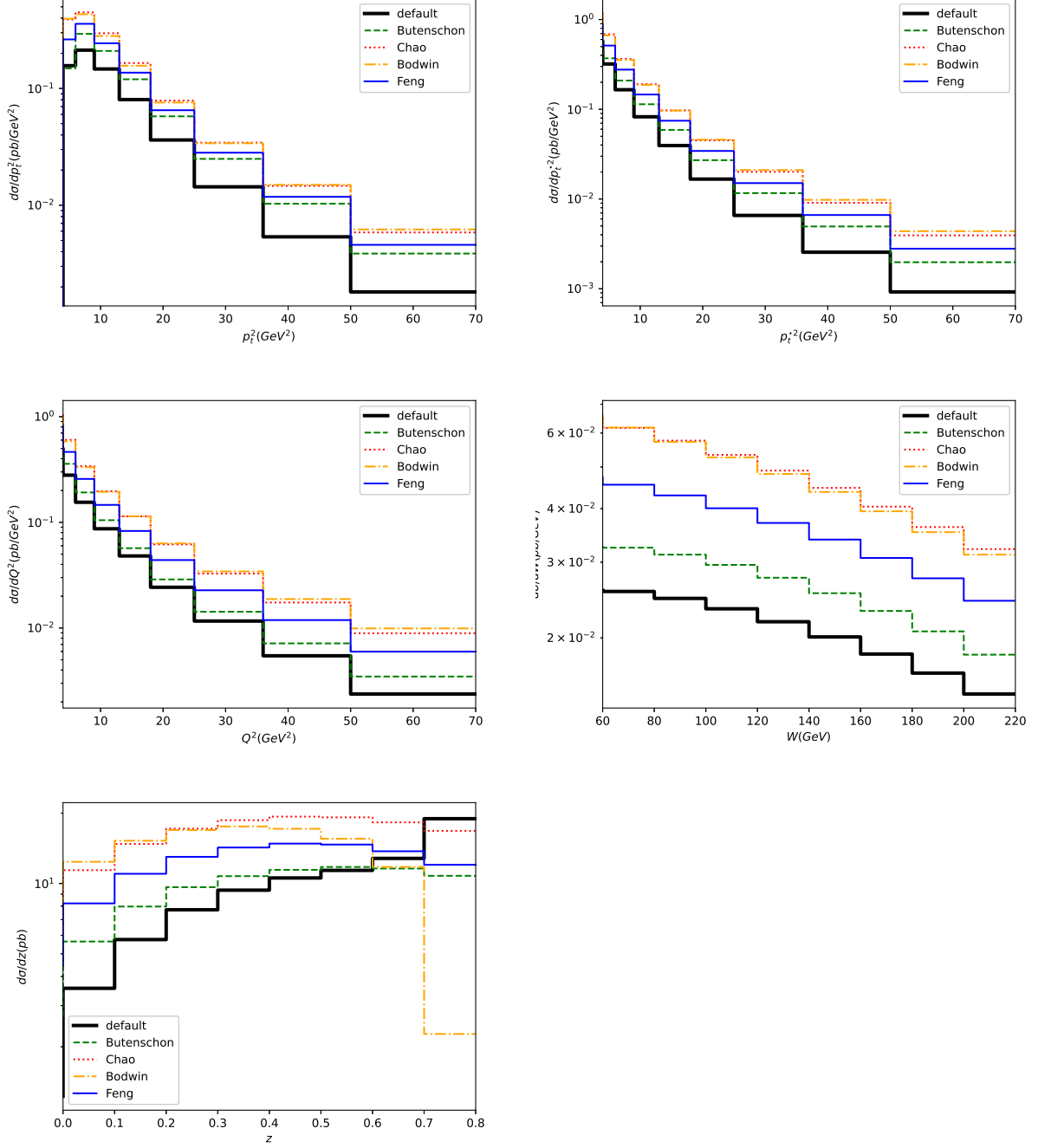


Figure 4: The differential cross sections of the η_c lepton production with respect to p_t^2 , p_t^{*2} , Q^2 , W , and z in HERA experimental condition.

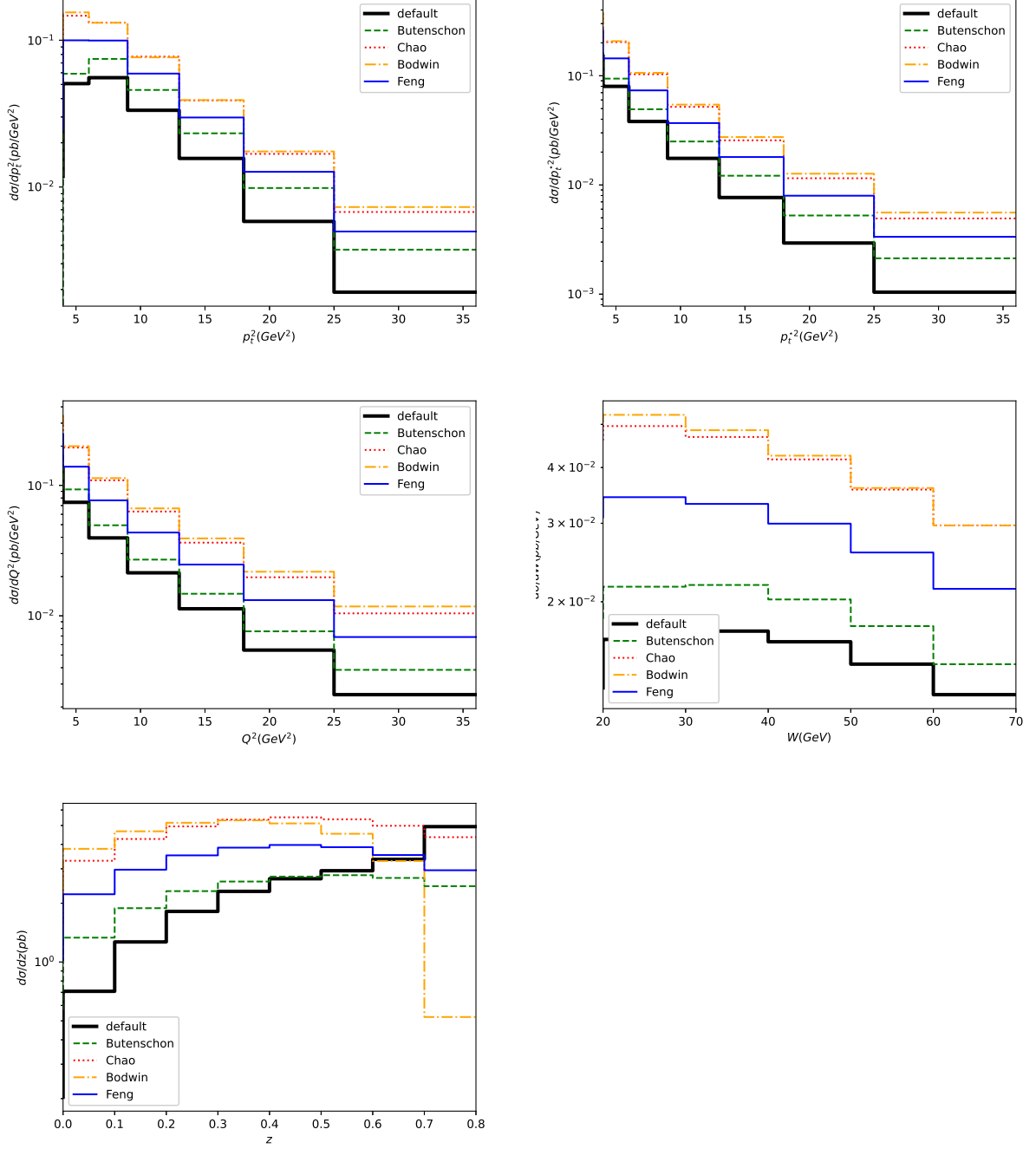


Figure 5: The differential cross sections of the η_c lepton production with respect to p_t^2 , p_t^{*2} , Q^2 , W , and z in HERA experimental condition.

Table 1: The colour-octet long-distance matrix elements for the η_c production obtained by different theory groups, where the relations between the LDMEs for the J/ψ and η_c production are employed.

References	Butenschon and <i>et al.</i> [8]	Chao and <i>et al.</i> [10]	Bodwin and <i>et al.</i> [30]	Feng and <i>et al.</i> [31]
$\langle \mathcal{O}^{\eta_c}(^1S_0^{[1]}) \rangle (\text{GeV}^3)$	0.44	0.387	0.387	0.387
$\langle \mathcal{O}^{\eta_c}(^1S_0^{[8]}) \rangle (10^{-2} \text{GeV}^3)$	0.056 ± 0.015	0.10 ± 0.04	-0.238 ± 0.121	0.059 ± 0.019
$\langle \mathcal{O}^{\eta_c}(^3S_1^{[8]}) \rangle (10^{-2} \text{GeV}^3)$	3.04 ± 0.35	8.9 ± 0.98	11.0 ± 1.4	5.66 ± 0.47
$\langle \mathcal{O}^{\eta_c}(^1P_1^{[8]}) \rangle / m_c^2 (10^{-2} \text{GeV}^3)$	-1.21 ± 0.21	1.68 ± 0.63	-0.936 ± 0.453	1.03 ± 0.31

4 Summary

In this paper, we study the η_c leptonproduction at the HERA and the future EIC. The nonrelativistic-QCD results for this process are obtained for the first time. Owing to the off-shell initial photon, the calculation of this process is actually very complicated. Having got the short-distance coefficients for the $c\bar{c}^1S_0^{[1]}$, $c\bar{c}^1S_0^{[8]}$, $c\bar{c}^3S_1^{[8]}$, and $c\bar{c}^1P_1^{[8]}$ production, we presented the differential cross sections for the η_c leptonproduction with respect to p_t^2 , p_t^{*2} , Q^2 , W , and z . Unlike the η_c photoproduction, in this process, the contributions from the colour-singlet channel is important, which is mainly due to a next-to-leading-power term rising from the off-shell initial photon. The four channels can be well distinguished by studying different kinematic distributions. By varying the scales (m_c , μ_r , and μ_f), we find the cross section is just slight dependent on them. At the end of this paper, we presented the results for different sets of long-distance matrix elements, and find that this process can provide a good opportunity to distinguish them.

Acknowledgments

This work is supported by the National Natural Science Foundation of China (Grant No. 11965006).

References

- [1] G. T. Bodwin, E. Braaten, and G. P. Lepage, *Rigorous QCD analysis of inclusive annihilation and production of heavy quarkonium*, *Phys. Rev.* **D51** (1995) 1125–1171, [[hep-ph/9407339](#)]. [Erratum: *Phys. Rev.*D55,5853(1997)].
- [2] CDF Collaboration, F. Abe et al., *Inclusive J/ψ , $\psi(2S)$ and b quark production in $\bar{p}p$ collisions at $\sqrt{s} = 1.8 \text{ TeV}$* , *Phys. Rev. Lett.* **69** (1992) 3704–3708.
- [3] E. Braaten and S. Fleming, *Color octet fragmentation and the psi-prime surplus at the Tevatron*, *Phys. Rev. Lett.* **74** (1995) 3327–3330, [[hep-ph/9411365](#)].
- [4] CDF Collaboration, A. Abulencia et al., *Polarization of J/ψ and ψ_{2S} Mesons Produced in $\bar{p}p$ Collisions at $\sqrt{s} = 1.96\text{-TeV}$* , *Phys. Rev. Lett.* **99** (2007) 132001, [[arXiv:0704.0638](#)].

- [5] Y.-Q. Ma, K. Wang, and K.-T. Chao, $J/\psi(\psi')$ production at the Tevatron and LHC at $\mathcal{O}(\alpha_s^4 v^4)$ in nonrelativistic QCD, *Phys. Rev. Lett.* **106** (2011) 042002, [[arXiv:1009.3655](#)].
- [6] M. Butenschoen and B. A. Kniehl, Reconciling J/ψ production at HERA, RHIC, Tevatron, and LHC with NRQCD factorization at next-to-leading order, *Phys. Rev. Lett.* **106** (2011) 022003, [[arXiv:1009.5662](#)].
- [7] Y.-Q. Ma, K. Wang, and K.-T. Chao, A complete NLO calculation of the J/ψ and ψ' production at hadron colliders, *Phys. Rev.* **D84** (2011) 114001, [[arXiv:1012.1030](#)].
- [8] M. Butenschoen and B. A. Kniehl, World data of J/ψ production consolidate NRQCD factorization at NLO, *Phys. Rev.* **D84** (2011) 051501, [[arXiv:1105.0820](#)].
- [9] M. Butenschoen and B. A. Kniehl, J/ψ polarization at Tevatron and LHC: Nonrelativistic-QCD factorization at the crossroads, *Phys. Rev. Lett.* **108** (2012) 172002, [[arXiv:1201.1872](#)].
- [10] K.-T. Chao, Y.-Q. Ma, H.-S. Shao, K. Wang, and Y.-J. Zhang, J/ψ Polarization at Hadron Colliders in Nonrelativistic QCD, *Phys. Rev. Lett.* **108** (2012) 242004, [[arXiv:1201.2675](#)].
- [11] B. Gong, L.-P. Wan, J.-X. Wang, and H.-F. Zhang, Polarization for Prompt J/ψ and $\psi(2s)$ Production at the Tevatron and LHC, *Phys. Rev. Lett.* **110** (2013), no. 4 042002, [[arXiv:1205.6682](#)].
- [12] Z. Sun and H.-F. Zhang, Reconciling charmonium production and polarization data in the midrapidity region at hadron colliders within the nonrelativistic QCD framework, *Chin. Phys.* **C42** (2018), no. 4 043104, [[arXiv:1505.02675](#)].
- [13] S. Barsuk, J. He, E. Kou, and B. Viaud, Investigating charmonium production at LHC with the $p\bar{p}$ final state, *Phys.Rev.* **D86** (2012) 034011, [[arXiv:1202.2273](#)].
- [14] **LHCb** Collaboration, R. Aaij et al., Measurement of the $\eta_c(1S)$ production cross-section in proton-proton collisions via the decay $\eta_c(1S) \rightarrow p\bar{p}$, *Eur. Phys. J.* **C75** (2015), no. 7 311, [[arXiv:1409.3612](#)].
- [15] H. Han, Y.-Q. Ma, C. Meng, H.-S. Shao, and K.-T. Chao, η_c production at LHC and indications on the understanding of J/ψ production, *Phys. Rev. Lett.* **114** (2015), no. 9 092005, [[arXiv:1411.7350](#)].
- [16] H.-F. Zhang, Z. Sun, W.-L. Sang, and R. Li, Impact of η_c hadroproduction data on charmonium production and polarization within NRQCD framework, *Phys. Rev. Lett.* **114** (2015), no. 9 092006, [[arXiv:1412.0508](#)].
- [17] **Belle** Collaboration, P. Pakhlov et al., Measurement of the $e^+e^- \rightarrow J/\psi c\bar{c}$ cross section at $s^{*(1/2)} \sim 10.6\text{-GeV}$, *Phys. Rev. D* **79** (2009) 071101, [[arXiv:0901.2775](#)].
- [18] Y.-J. Li, G.-Z. Xu, P.-P. Zhang, Y.-J. Zhang, and K.-Y. Liu, Study of Color Octet Matrix Elements Through J/ψ Production in e^+e^- Annihilation, *Eur. Phys. J. C* **77** (2017), no. 9 597, [[arXiv:1409.2293](#)].
- [19] H. Haberzettl and J. P. Lansberg, Possible solution of the J/ψ production puzzle, *Phys. Rev. Lett.* **100** (2008) 032006, [[arXiv:0709.3471](#)].
- [20] Y.-Q. Ma, Y.-J. Zhang, and K.-T. Chao, QCD correction to $e^+e^- \rightarrow J/\psi + gg$ at B Factories, *Phys. Rev. Lett.* **102** (2009) 162002, [[arXiv:0812.5106](#)].
- [21] B. Gong and J.-X. Wang, Next-to-Leading-Order QCD Corrections to $e^+e^- \rightarrow J/\psi gg$ at the B Factories, *Phys. Rev. Lett.* **102** (2009) 162003, [[arXiv:0901.0117](#)].

- [22] B. Gong and J.-X. Wang, *Next-to-leading-order QCD corrections to $e+e^- \rightarrow J/\psi(cc)$ at the B factories*, *Phys. Rev. D* **80** (2009) 054015, [[arXiv:0904.1103](#)].
- [23] H.-F. Zhang, Y. Feng, W.-L. Sang, and Y.-P. Yan, *Kinematic distributions of the η_c photoproduction in ep collisions within the nonrelativistic QCD framework*, *Phys. Rev. D* **99** (2019), no. 11 114018, [[arXiv:1902.09056](#)].
- [24] L.-K. Hao, F. Yuan, and K.-T. Chao, *Inelastic electroproduction of η_c at ep colliders*, *Phys. Rev. D* **62** (2000) 074023, [[hep-ph/0004203](#)].
- [25] H.-F. Zhang and Z. Sun, *Leptonic current structure and azimuthal asymmetry in deeply inelastic scattering*, *Phys. Rev. D* **96** (2017), no. 3 034002, [[arXiv:1701.08728](#)].
- [26] Z. Sun and H.-F. Zhang, *QCD leading order study of the J/ψ leptonproduction at HERA within the nonrelativistic QCD framework*, *Eur. Phys. J. C* **77** (2017), no. 11 744, [[arXiv:1702.02097](#)].
- [27] Z. Sun and H.-F. Zhang, *QCD corrections to the color-singlet J/ψ production in deeply inelastic scattering at HERA*, *Phys. Rev. D* **96** (2017), no. 9 091502, [[arXiv:1705.05337](#)].
- [28] P. Artoisenet, J. M. Campbell, F. Maltoni, and F. Tramontano, *J/ψ production at HERA*, *Phys. Rev. Lett.* **102** (2009) 142001, [[arXiv:0901.4352](#)].
- [29] J. Pumplin, D. R. Stump, J. Huston, H. L. Lai, P. M. Nadolsky, and W. K. Tung, *New generation of parton distributions with uncertainties from global QCD analysis*, *JHEP* **07** (2002) 012, [[hep-ph/0201195](#)].
- [30] G. T. Bodwin, K.-T. Chao, H. S. Chung, U.-R. Kim, J. Lee, and Y.-Q. Ma, *Fragmentation contributions to hadroproduction of prompt J/ψ , χ_{cJ} , and $\psi(2S)$ states*, *Phys. Rev.* **D93** (2016), no. 3 034041, [[arXiv:1509.07904](#)].
- [31] Y. Feng, B. Gong, C.-H. Chang, and J.-X. Wang, *The remaining parts for the long-standing J/ψ polarization puzzle*, *Phys. Rev.* **D99** (2019), no. 1 014044, [[arXiv:1810.08989](#)].
- [32] G. T. Bodwin, H. S. Chung, U.-R. Kim, and J. Lee, *Fragmentation contributions to J/ψ production at the Tevatron and the LHC*, *Phys. Rev. Lett.* **113** (2014), no. 2 022001, [[arXiv:1403.3612](#)].